

Phase Equilibrium, Volumetric, and Interfacial Properties of the Ionic Liquid, 1-Hexyl-3-methylimidazolium Bis(trifluoromethylsulfonyl)amide and 1-Octene

Azita Aghosseini, Brent Sensenich,[†] Laurence R. Weatherley, and Aaron M. Scurto*

Department of Chemical & Petroleum Engineering and NSF-ERC Center for Environmentally Beneficial Catalysis, University of Kansas, Lawrence, Kansas 66045

Biphasic systems involving ionic liquids (ILs) form the basis of many applications in extractions and reactions. In this work, the liquid–liquid phase equilibrium, density, molar volume, excess molar volume, and interfacial and surface tensions are measured for saturated and subsaturated mixtures of 1-hexyl-3-methylimidazolium bis(trifluoromethylsulfonyl)amide ([HMIm][Tf₂N]) and 1-octene at four different temperatures, (10, 25, 50, and 75) °C. Many of the properties of the IL phase change significantly with the increasing concentration of 1-octene. The nonrandom two-liquid (NRTL) activity coefficient model was utilized to model the mutual solubility of two liquids. 1-Octene is fairly soluble in the [HMIm][Tf₂N], but the IL solubility in the 1-octene is very small. The excess molar volume for the mixture of ILs and 1-octene is slightly negative for all isotherms and becomes more negative with an increase in temperature. The air–liquid surface tension decreases with increasing 1-octene concentration, and the saturated [HMIm][Tf₂N] + 1-octene interfacial tension decreases significantly at higher temperatures.

1. Introduction

Numerous applications of ionic liquids (ILs) have been demonstrated in the literature and industry. The physico-chemical properties of ILs can be molecularly designed to positively affect reactions, extractions, and materials processing. In addition, their lack of significant vapor pressure eliminates potential air pollution, which is a considerable advantage over conventional organic solvents. Many current and potential applications utilize ILs in biphasic scenarios, for example, liquid–liquid, liquid–vapor, liquid–solid, and so forth. For instance, biphasic extractions and reactions have been reported.^{1–3} As with any multiphase system, a quantitative understanding of the phase equilibrium thermodynamics, mass transport properties, and interphase mass transfer rates are necessary to properly design and understand these systems. However, only limited data in any one of these areas is currently available in the literature.

We have recently initiated a complete study of biphasic mass transfer in a model system of 1-*n*-hexyl-3-methylimidazolium bis(trifluoromethylsulfonyl)amide ([HMIm][Tf₂N]) and 1-octene (see Figure 1). [HMIm][Tf₂N] is a common IL and chosen as a model IL by the IL working group of IUPAC.⁴ We have utilized [HMIm][Tf₂N] in various systems for homogeneously catalyzed reactions^{5,6} and in phase equilibria and extractions.^{7,8} As will be discussed below, the solubility of [HMIm][Tf₂N] in 1-octene is very small, but the 1-octene solubility in the IL phase is moderate. Thus, mass transfer will occur in virtually one direction and thus simplify the mass transfer study in the biphasic system. However, to model the mass transfer of 1-octene into the IL under certain flow conditions, for example, falling IL droplets, and so forth, the complete concentration and temperature dependent thermodynamic and mass transport

properties must be known. Olefin and IL systems have applications in olefin extraction^{9,10} and catalysis (hydroformylation, hydrogenation, and so forth).^{5,11–13}

In this work, thermodynamic properties of liquid–liquid equilibrium, density, and interfacial and surface tension are measured for the system of 1-hexyl-3-methylimidazolium bis(trifluoromethylsulfonyl)amide ([HMIm][Tf₂N]) and 1-octene. Focus is placed on quantifying the effect of 1-octene concentration on these various properties.

2. Experimental Methods

2.1. Synthesis of the ILs. 1-Hexyl-3-methylimidazolium bis(trifluoromethylsulfonyl)amide ([HMIm][Tf₂N]) was prepared by anion exchange from the corresponding bromide salt of the imidazolium cation ([HMIm][Br]) with lithium bis(trifluoromethylsulfonyl)amide (Li[Tf₂N]) in deionized water as described in the literature.^{14,15} The bromide salt of the imidazolium cation was prepared from a quaternization reaction of 1-methylimidazole with a slight excess amount of the corresponding 1-bromohexane in acetonitrile at 40 °C under an argon atmosphere with stirring for three days. *Caution: This reaction is highly exothermic, and adequate solvent volumes and/or cooling must be provided during the reaction.* The bromide salt of 1-hexyl-3-methylimidazolium was purified with activated charcoal (10 %), stirring for 24 h. Acetonitrile was added to reduce the viscosity of the IL, and the mixture was filtered. The mixture was then passed through a plug of Celite (depth = 7 cm, diameter = 3 cm) and through a short column (height = 20 cm, diameter = 2.5 cm) of acidic alumina. The solvent was removed on a rotary evaporator under reduced pressure at 40 °C and then connected to a high vacuum (< 0.013 Pa) at 50 °C for at least 48 h. [HMIm][Tf₂N] was synthesized by anion exchange between the [HMIm][Br] and the Li[Tf₂N]. The denser hydrophobic IL phase was decanted and washed with water for 6 to 8 times. The IL was then dried under vacuum at approximately 80 °C. Great care was taken to adequately remove any of the bromide impurities and water as these contaminants

* Corresponding author. Phone: +1 (785) 864-4947; fax: +1 (785) 864-4967; e-mail: ascurto@ku.edu.

[†] Current address: Neutrogena Corporation, 5760 W. 96th St., Los Angeles, CA 90054.

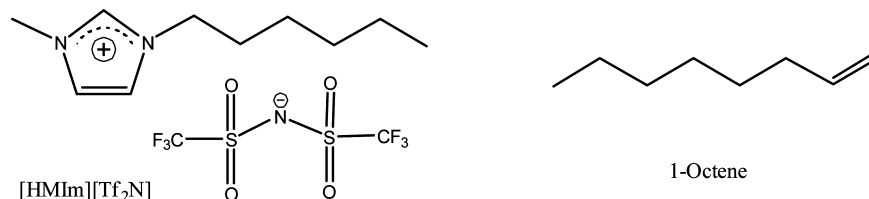


Figure 1. Structure of 1-*n*-hexyl-3-methylimidazolium bis(trifluoromethylsulfonyl)amide ([HMIm][Tf₂N]) and 1-octene.

may significantly change the physical properties.¹⁶ The purified samples were stored and handled in Schlenk tubes and procedures under dry argon.

¹H NMR chemical shifts (relative to TMS internal standard) and coupling constants J/Hz : δ = 8.65 (s, 1H), 7.39 (d, 2H, J = 4.19), 4.17 (q, 2H, J = 7.4), 3.93 (s, 3H), 1.87 (m, 4H), 1.32 (6H, m) 0.87 (t, 3H, J = 6.53). Analysis calculated for C₁₂H₁₉N₃F₆S₂O₄: C, 32.2; H, 4.28; N, 9.39; S, 14.33. Found: C, 32.21; H, 4.27; N, 9.25; S, 14.19. From NMR and elemental analysis, the estimated purity is 99 + %. The residual bromide mass fraction is less than $8 \cdot 10^{-6}$, and the water mass fraction was always less than $3.5 \cdot 10^{-4}$.

2.2. Phase Equilibrium Measurements. The liquid–liquid equilibrium envelope at ambient pressure of 1-octene and the IL was determined in this study. The amount of 1-octene in [HMIm][Tf₂N] was measured by a cloud-point method where one component was continuously yet slowly added to the other component until the mixture became cloudy. The amount of each pure component was measured with a Mettler Toledo XS205 dual range balance, with an accuracy of 0.01 mg for the range as a maximum of 81 g and 0.1 mg for the range as a maximum of 220 g. A Branson model 2510 ultrasonic bath was used to mix the solutions. Temperature control at (10 and 25) °C was provided by a Fisher Scientific Isotemp 3016 circulating chiller with a resolution of ± 0.1 °C. For higher temperatures, samples were heated and stirred on an aluminum vial holder on an IKA RET basic C hot plate with ETS-D4 fuzzy logic controller and resolution of ± 0.1 °C. To prevent the loss of 1-octene because of evaporation, a septum cap was used.

The amount of [HMIm][Tf₂N] in the octene phase was measured by inductively coupling plasma/optical emission spectroscopy (ICP-OES; Jobin-Yvon-Horiba JY2000). The ICP-OES is very sensitive to sulfur concentration as found in the anion, even in nonaqueous solvents as configured here. The IL and 1-octene were mixed and stirred for one day (24 h) at the four different isotherms (10 °C, 25 °C, 50 °C, or 75 °C) using an oil bath with the temperature controller above. Four samples were taken from the 1-octene phase and mixed with ethanol to maintain a single phase at ambient temperature. Volumetric pipettes and flasks were used for all measurements. The samples were analyzed using the ICP-OES for the sulfur concentration which is in the anion.

2.3. Density. Density was measured using an Anton Parr densitometer (DMA 4500) which is based on U-tube oscillation. To perform a measurement, the sample was loaded into the measuring cell. Excess sample was used to first purge the U-tube of air and then to provide an accurate solution in the measuring cell. Uncertainty is within $\pm 0.0001 \text{ g} \cdot \text{cm}^{-3}$. The system was periodically checked with distilled water at 20 °C.

2.4. Surface and Interfacial Tension. The Krüss EasyDyne tensiometer was used in this work to measure surface tension and interfacial tension of the liquids. Temperature was maintained with the Krüss thermoset jacket TJ1020 connected to a laboratory circulating pump. The instrument can operate in a temperature range of (−10 to 100) °C with the resolution of

± 0.1 °C. Measuring range for surface and interfacial tensions was between (1 and 999) mN·m^{−1} with a resolution of ± 0.1 mN·m^{−1}. The unit operates using the ring method where a platinum/iridium alloy ring immersed below either the liquid (for surface tension) or below the liquid–liquid interface (for interfacial tension) is raised slowly while measuring the force. The force required to raise the ring just at the interface is at a maximum. This maximum force is directly related to the surface or interfacial tension with knowledge of the density. Ten measurements were taken and reported together with the average value and the standard deviation. The surface tension of deionized water at 25 °C was measured as 69.0 mN·m^{−1} which compared with a literature report¹⁷ of 71.99 mN·m^{−1}. The interfacial tension between octane and water was measured as 51.0 mN·m^{−1} compared with 51.2 mN·m^{−1} from Zeppieri et al.¹⁸

2.5. Analysis. Elemental analysis was performed by Desert Analytics Transwest Geochem. ¹H NMR spectra were recorded on a Bruker 400 NMR spectrometer using trimethylsilyl (TMS) as a reference for ¹H chemical shifts. Gas chromatography analyses of the product mixtures were carried out on a Varian CP-3800 series gas chromatograph equipped with a flame ionization detector (GC-FID for quantitative analyses) and a chrompack capillary column CP-Sil 5 CB (25 m, 0.32 mm, 1.2 μm). The water content was determined by a Mettler Toledo DL32 Karl Fisher coulometer, and the Br content was measured by a Cole Parmer bromide electrode (27502-05) read with an Oakton Ion 510 series meter. The amount of IL in the 1-octene phase at different isotherms was measured using Jobin-Yvon ICP-OES spectrometer (JY 2000) by following the sulfur emissions from the anion in a nonaqueous solvent (ethanol). The ICP parameters were: power = 1350 W; argon pressure = 620.5 kPa for plasma and nebulizer; plasma flow: 18 L·min^{−1}; sheath flow; 0.8 L·min^{−1}; auxiliary flow = 0.3 L·min^{−1}; nebulizer type = concentric glass nebulizer; nebulizer flow = 1.63 L·min^{−1}; nebulizer pressure 1.19 bar; and sample pump flow = 0.3 mL·min^{−1}.

2.6. Materials. Argon (extra dry grade, 99.998 %) was obtained from Airgas, Inc. 1-Octene (CAS 111-66-0), 98 %, 1-methylimidazole, (CAS 616-47-7), 99 + %, lithium bis(trifluoromethylsulfonyl)amide (CAS 90076-65-6), 99.95 %, and acetonitrile (CAS 75-05-8), ≥ 99.9 %, were purchased from Sigma-Aldrich. 1-Bromohexane (CAS 111-25-1), 99 + %, was obtained from Acros. 1-Methyl-imidazole and 1-bromohexane were vacuum-distilled and used immediately in the synthesis.

2.7. Modeling. The NRTL (nonrandom two-liquid) activity coefficient model¹⁹ was utilized to correlate the experimental data. The equations are given as:

$$\ln \gamma_1 = x_2^2 \left[\tau_{21} \left(\frac{G_{21}}{x_1 + x_2 G_{21}} \right)^2 + \frac{\tau_{12} G_{12}}{(x_2 + x_1 G_{12})^2} \right] \quad (1)$$

$$\ln \gamma_2 = x_1^2 \left[\tau_{12} \left(\frac{G_{12}}{x_2 + x_1 G_{12}} \right)^2 + \frac{\tau_{21} G_{21}}{(x_1 + x_2 G_{21})^2} \right] \quad (2)$$

$$G_{12} = \exp(-\alpha_{12}\tau_{21}) \quad (3)$$

$$G_{21} = \exp(-\alpha_{12}\tau_{12}) \quad (4)$$

where α_{12} is related to nonrandomness in the mixture and is set equal to 0.2. The binary interaction parameters (BIPs), τ_{12} and τ_{21} , were fitted to the data at each temperature using CHEMCAD software version 6.1.2 and using the BIP regression algorithm (Complex method) and the objective function:

$$\min \sum_{p=1}^2 \sum_{i=1}^{NP} (x_i^{p,\text{calc}} - x_i^{p,\text{exp}})^2 \quad (5)$$

3. Results and Discussion

3.1. Liquid–Liquid Equilibrium. The mutual solubility of 1-octene and [HMIm][Tf₂N] was measured at (10, 25, 50, and 75) °C, and the values are listed in Table 1. The uncertainties of Table 1 represent the standard deviations in the cloud point measurement with at least three replications. For the IL in the octene, the uncertainties are from the propagation of the standard deviations in the ICP-OES signal on the resulting mole fraction solubility. As shown in Figure 2, appreciable quantities of the 1-octene are soluble in the IL phase. For instance at 25 °C, the solubility is approximately 0.2 mole fraction. However, the solubility of [HMIm][Tf₂N] in 1-octene was very low (< 0.0001 mole fraction). Even at 75 °C, the solubility of the IL in the 1-octene phase is only about 0.045 mole fraction. This produces a highly asymmetric liquid–liquid region. This general phase behavior has interesting ramifications for mass transfer in a biphasic system. When 1-octene and [HMIm][Tf₂N] are contacted, mass transfer will only be in virtually one direction especially at lower temperatures, that is, 1-octene dissolution in [HMIm][Tf₂N]. The NRTL model was used to correlate the data. The model accurately correlates the 1-octene mutual solubility data at the temperatures investigated, albeit with slight undercorrelation of the 1-octene solubility in each phase. The model performance and BIPs are listed in Table 2.

There are a few studies in literature for n-alkene solubility in ILs.^{20–22} Stark et al.²³ determined the relative solubility of

Table 2. Regressed NRTL Parameters and Performance for the Solution of Mixtures of 1-Octene (1) + [HMIm][Tf₂N] (2)

	<i>t</i> /°C			
	10	25	50	75
τ_{12}	4.8985	3.8672	3.7535	3.1465
τ_{21}	0.3532	0.3354	0.3095	0.291
dev. ^a (x_1^I)	−0.0053	−0.0174	−0.0288	−0.0168
dev. ^a (x_1^{II})	−0.0043	−0.0074	−0.019	−0.0135
AARD ^b (x_1^I)	0.0775			
AARD ^b (x_1^{II})	0.0112			

^a Deviation = $(x_1^{p,\text{pred}} - x_1^p)$.

^b

$$\text{AARD} = \frac{1}{N} \sum_{i=1}^N \left[\left| \frac{x_1^{I,\text{pred}}(T_i) - x_1^I(T_i)}{x_1^I(T_i)} \right| + \left| \frac{x_1^{II,\text{pred}}(T_i) - x_1^{II}(T_i)}{x_1^{II}(T_i)} \right| \right]$$

1-octene in several imidazolium ILs and showed that the solubility increases with the cation of 1-butyl-3-methylimidazolium ([BMIm]) in the order of: [BF₄] < [PF₆] < [OTf] < [Tf₂N] where [OTf] is the trifluoromethylsulfonate anion. However, they do not report the quantitative solubility. They also showed that for a given anion, longer alkyl chains yield a higher solubility of 1-octene. Other reports indicate that the smaller 1-hexene is slightly more soluble in ILs than 1-octene.^{20,22,24,25} For instance, the solubility of 1-hexene in [BMIm][PF₆] at 30 °C is approximately 0.12 mole fraction.²⁶ Most imidazolium ILs have much larger solubility for olefins compared with alkanes as the solubility of *n*-hexane in [BMIm][PF₆] at 41.3 °C is 0.058 mole fraction.²⁵ However, the solubility of most imidazolium ILs in the alkene or alkane phase is very low: usually much less than 0.01 mole fraction at ambient conditions.²⁷ This large difference in alkene/alkane solubility and low solubility of the IL is being exploited for olefin extraction.^{28,29}

The molar excess enthalpy, H^E , can be computed from the NRTL activity coefficient/ G^E model from the regressed parameters.

$$H^E = G^E - T \left(\frac{\partial G^E}{\partial T} \right)_{P,x} \quad (6)$$

From this relationship, the excess enthalpy is positive throughout the composition range and indicates that mixing is endothermic.^{30–33} The model predicts that the excess enthalpy increases with temperature at a given composition. Nebig et al.³⁰ measured the excess enthalpy for this [HMIm][Tf₂N] + 1-octene system at 140 °C and found that the excess enthalpy is positive at this much elevated temperature.

3.2. Density. While the density of many different pure ILs has been extensively studied, fewer studies exist for mixtures. In this work, the density of pure and mixtures of [HMIm][Tf₂N] and 1-octene to their saturation point was measured at (10, 25, 50, and 75) °C and listed in Table 3. The density of pure [HMIm][Tf₂N] is reported in literature at different temperatures from several sources. At 75 °C, the maximum absolute deviation between the literature sources is 0.0029 g·cm^{−3}.^{34,35} For pure 1-octene at 25 °C, the reported density is 0.711 g·cm^{−3},³⁶ which is exactly equal to our result. The density of the IL decreases with the increasing mole fraction of 1-octene as seen in Figure 3. The change is not a strictly linear decrease. At 75 °C, the density difference between pure [HMIm][Tf₂N] and a mixture of [HMIm][Tf₂N] with a mole fraction of 0.28 1-octene (saturation) is only approximately −4.3 %. The temperature dependence of density at each composition is linearly dependent between (10 and 75) °C and shown in Figure 4.

Table 1. Experimental Liquid–Liquid Equilibrium of 1-Octene (1) + [HMIm][Tf₂N] (2)

<i>t</i> /°C	x_1^{IIa}	x_1^{Ib}
10	0.16 ± 0.01	0.9999 ± 0.0001
25	0.19 ± 0.01	0.9999 ± 0.0004
50	0.23 ± 0.02	0.9986 ± 0.0009
75	0.28 ± 0.02	0.9552 ± 0.0008

^a x_1^{II} is the [HMIm][Tf₂N]-rich phase. ^b x_1^I indicates the 1-octene-rich phase.

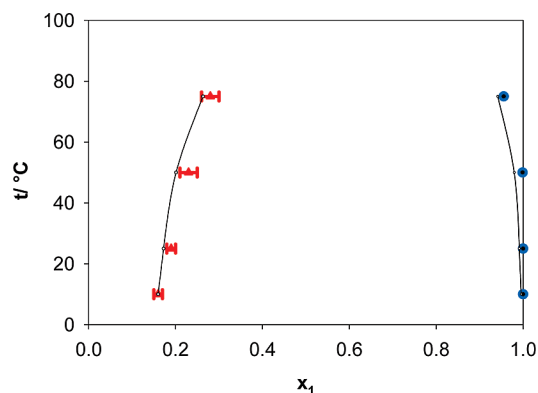
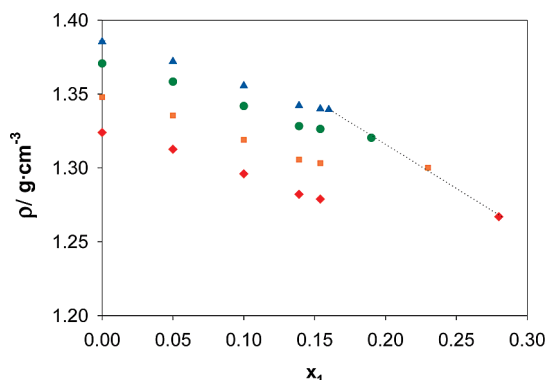
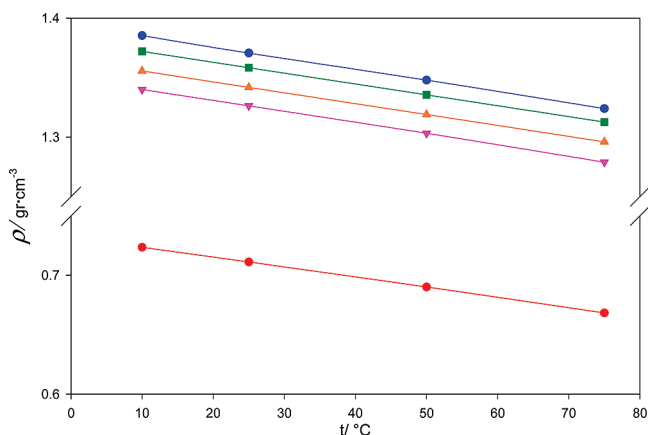


Figure 2. Liquid–liquid equilibrium of 1-octene (1) + [HMIm][Tf₂N] (2). The line is the correlation by the NRTL model.

Table 3. Density of Mixtures of 1-Octene (1) + [HMIm][Tf₂N] (2)

x_1	density ρ [g·cm ⁻³]			
	10 °C	25 °C	50 °C	75 °C
0	1.3854 ± 0.0004	1.3707 ± 0.0006	1.348 ± 0.002	1.324 ± 0.002
0.05 ± 0.0001	1.3721 ± 0.0008	1.358 ± 0.006	1.336 ± 0.002	1.313 ± 0.005
0.10 ± 0.0001	1.356 ± 0.005	1.342 ± 0.002	1.319 ± 0.006	1.30 ± 0.01
0.139 ± 0.0001	1.34 ± 0.01	1.328 ± 0.007	1.306 ± 0.006	1.282 ± 0.006
0.154 ± 0.0001	1.34 ± 0.01	1.326 ± 0.003	1.303 ± 0.002	1.279 ± 0.011
0.16 ^a ± 0.01	1.340 ± 0.009			
0.19 ^a ± 0.01		1.3204 ± 0.0001		
0.23 ^a ± 0.02			1.300 ± 0.002	
0.28 ^a ± 0.02				1.267 ± 0.012
1.0	0.7235 ± 0.0006	0.7112 ± 0.0006	0.69 ± 0.01	0.668 ± 0.012

^a This number reflects the saturation value at each isotherm.**Figure 3.** Density of 1-octene (1) + [HMIm][Tf₂N] (2). Dashed line indicates saturation limit. ▲, 10 °C; ●, 25 °C; ■, 50 °C; ◆, 75 °C.**Figure 4.** Density of the 1-octene (1) + [HMIm][Tf₂N] (2) with temperature and composition of 1-octene. Line is of smoothed data. 1-octene mole fraction, x_1 : ●, 0; ■, 0.05; ▲, 0.1; ▼, 0.154; ◆, 1.

3.2.1. Excess Molar Volume. From the density data and the composition of the mixture, the excess molar volume (V^E) can be computed from:

$$V^E = V_m - x_1 V_1 - x_2 V_2 = \frac{x_1 M_1 + x_2 M_2}{\rho_m} - \frac{x_1 M_1}{\rho_1} - \frac{x_2 M_2}{\rho_2} \quad (7)$$

where V_i and ρ_i are the molar volumes and densities, respectively, of pure 1-octene (1), pure [HMIm][Tf₂N] (2), and their mixture (m), respectively; M_i and x_i are their molar masses and mole fractions of component i , respectively. A full error analysis was performed to determine the inherent errors in the excess molar volume at each point; the maximum uncertainty for excess molar volume is about 0.2 cm³·mol⁻¹ (Table 4). Excess molar

Table 4. Excess Molar Volume of Mixtures of 1-Octene (1) + [HMIm][Tf₂N] (2) at Four Temperatures

x_1	$t = 10$ °C			
	V_m cm ³ ·mol ⁻¹	±	V^E cm ³ ·mol ⁻¹	±
0	322.93	0.02	0	
0.05 ± 0.0001	313.85	0.14	-0.69	0.14
0.1 ± 0.0001	305.29	0.13	-0.85	0.14
0.139 ± 0.0001	298.62	0.13	-0.98	0.14
0.154 ± 0.0001	295.35	0.13	-1.73	0.14
0.16 ^a ± 0.01	293.97	0.13	-2.11	0.14
1	155.08	0.02	0	
x_1	$t = 25$ °C			
	V_m cm ³ ·mol ⁻¹	±	V^E cm ³ ·mol ⁻¹	±
0	326.40	0.03	0	
0.05 ± 0.0001	317.03	0.14	-0.94	0.15
0.1 ± 0.0001	308.44	0.14	-1.10	0.19
0.139 ± 0.0001	301.75	0.14	-1.22	0.19
0.154 ± 0.0001	298.41	0.14	-2.03	0.19
0.19 ^a ± 0.01	290.61	0.03	-3.76	0.13
1	157.77	0.03	0	
x_1	$t = 50$ °C			
	V_m cm ³ ·mol ⁻¹	±	V^E cm ³ ·mol ⁻¹	±
0	331.92	0.03	0	
0.05 ± 0.0001	322.45	0.15	-1.01	0.20
0.1 ± 0.0001	313.78	0.14	-1.21	0.14
0.139 ± 0.0001	307.00	0.14	-1.38	0.14
0.154 ± 0.0001	303.69	0.14	-2.15	0.14
0.23 ^a ± 0.02	284.82	0.13	-8.15	0.14
1	162.58	0.15	0	
x_1	$t = 75$ °C			
	V_m cm ³ ·mol ⁻¹	±	V^E cm ³ ·mol ⁻¹	±
0	337.92	0.15	0	
0.05 ± 0.0001	328.06	0.15	-1.35	0.21
0.1 ± 0.0001	319.35	0.15	-1.57	0.20
0.139 ± 0.0001	312.61	0.15	-1.68	0.20
0.154 ± 0.0001	309.47	0.15	-2.27	0.20
0.28 ^a ± 0.02	279.05	0.13	-11.26	0.20
1	167.89	0.15	0	

^a Saturated value.

volume of the solution indicates the deviation from ideal solution behavior at the same temperature and pressure.

As can be seen in Figure 5, the excess molar volume for the mixture of ILs and 1-octene is slightly negative for all isotherms below approximately 0.15 mole fraction of octene. Above this mole fraction, the excess molar volume becomes more negative until the saturation point is reached. The excess molar volume slightly increases (more negative) with temperature, ($\partial V^E / \partial T$)_{P,x} < 0; thus, these contraction effects become a bit more pronounced with temperature. These trends may indicate that, as small amounts of 1-octene are added, the intermolecular forces are dominated by IL–IL interactions and that the 1-octene may simply occupy the spaces between the ions or by weak dispersion interactions between the 1-hexyl- group of the cation and 1-octene. However, as the mixture becomes more concentrated in the 1-octene, the compounds may begin to have

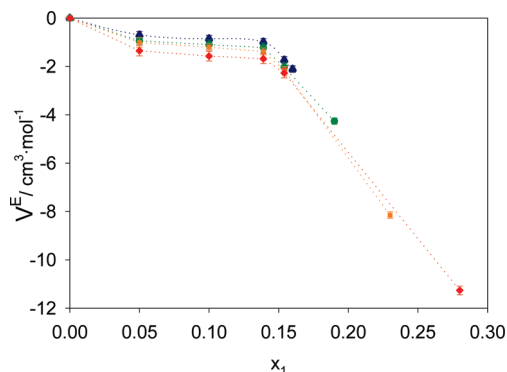


Figure 5. Excess molar volume of 1-octene (1) + [HMIm][Tf₂N] (2). The last point of the isotherm is the value at saturation. Smoothed line for visual aid. ▲, 10 °C; ●, 25 °C; ■, 50 °C; ◆, 75 °C.

Table 5. Surface Tension $\sigma/\text{mN}\cdot\text{m}^{-1}$ of 1-Octene (1) + [HMIm][Tf₂N](2) and Their Mixtures

x_1	10 °C	25 °C	50 °C	75 °C
0	31.2 ± 0.1	30.8 ± 0.2	28.9 ± 0.4	27.6 ± 0.2
0.05 ± 0.0001	30.9 ± 0.1	30.3 ± 0.1	28.8 ± 0.6	27.4 ± 0.3
0.1 ± 0.0001	29.8 ± 0.1	29.4 ± 0.0	28.7 ± 0.5	27.2 ± 0.6
0.15 ± 0.0001	27.8 ± 0.1	27.4 ± 0.1	26.6 ± 0.2	26.3 ± 0.6
0.16 ^a ± 0.01	27.7 ± 0.1			
0.19 ^a ± 0.01		27.0 ± 0.1		
0.23 ^a ± 0.02			25.5 ± 0.4	
0.28 ^a ± 0.02				25.3 ± 0.4
1	22.5 ± 0.1	21.2 ± 0.1	18.5 ± 0.1	15.7 ± 0.1

^a Reflects the saturation value at each isotherm.

stronger interactions possibly between the unsaturated regions of the cation and 1-octene, which results in a volume contraction.

Wang et al.^{37,38} also observed similar negative trends for the mixtures of [BMIm][PF₆] and organic compounds such as acetonitrile, dichloromethane, 2-butanone, and dimethylformamide. Heintz et al.³⁹ explained that the negative values of the molar excess volume between 4-methyl-*N*-butylpyridinium tetrafluoroborate [4MBP][BF₄] upon mixing with methanol molecules are most likely stabilized by ion–dipole interactions in the mixture. However, positive excess molar volumes have been reported for [BMIm][BF₄] + H₂O and [EMIm][BF₄] + H₂O mixtures by Seddon et al.¹⁶

In a recent experimental thermodynamic and molecular dynamics simulation study of CO₂ + imidazolium-based ILs by Cadena et al.,⁴⁰ it was suggested that the anions and cations of the ILs form a strong network with the interstices available in the fluid. Therefore, it is possible that the relatively small organic molecules fit into the interstices upon mixing. In addition, it was found from molecular dynamics simulations⁴¹ that the non-hydrogen bonding polar solutes, such as the organic compounds investigated in this work, interact much more strongly with the cations of the ILs by ion–dipole interactions. The filling effect of organic compounds in the interstices of ILs, and the ion–dipole interactions between the organic compound and the imidazolium ring of the ILs all contribute to the negative values of the molar excess volumes.

3.3. Surface Tension. There are several studies in the literature concerning surface tension of pure ILs. Huddleson et al.⁴² measured surface tension for several ILs and demonstrated that these values are higher than for organic solvents such as hexane and toluene but not as high as water at the same temperature. Law and Watson⁴³ also measured the surface tension of some *N*-alkylimidazolium ILs and showed the decreasing trend of these values with temperature. Dzyuba and Bartsch⁴⁴ studied the structural effect on surface tension for

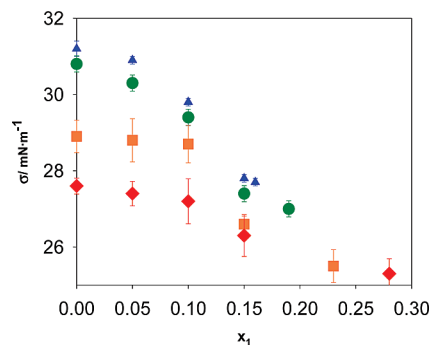


Figure 6. Surface tension of 1-octene (1) + [HMIm][Tf₂N] (2) and their mixtures. ▲, 10 °C; ●, 25 °C; ■, 50 °C; ◆, 75 °C.

Table 6. Interfacial Tensions and Model Interaction Parameters for 1-Octene (1) + [HMIm][Tf₂N] (2) at Different Temperatures

t °C	σ_{IT} mN·m ⁻¹	ϕ
10	13.3 ± 1.3	0.76
25	13.0 ± 1.3	0.76
50	9.7 ± 1.3	0.82
75	4.4 ± 1.3	0.93

some ILs and found that increasing the length of 1-alkyl chain on imidazolium cations decreases the surface tension. Freire et al.⁴⁵ also mentioned the effect of increasing alkyl chain of cations and its branching on decreasing surface tension of ILs. They also explain the effect of size of anions on the surface tension. The larger anions decrease the surface tension due to more charge delocalization resulting in weaker interactions between ions. The hydrogen bonding often increases surface tension because of the high cohesiveness and interactions between ions.⁴⁵

Here, we have measured the surface tension of mixtures of [HMIm][Tf₂N] and 1-octene to their saturation point at (10, 25, 50, and 75) °C, and the data are listed in Table 5. As can be seen from the result in Figure 6, the surface tension decreases as the 1-octene concentration increases; the pure component surface tension of 1-octene is much lower than the IL. However, this effect diminishes percentage wise at the higher temperatures. Kimura et al.⁴⁶ measured the surface tension of 1-octene (23.4 mN·m⁻¹ at 20 °C), which was close to the value that Jasper⁴⁷ reported (21.8 mN·m⁻¹) compared with our data at 25 °C of 21.2 mN·m⁻¹. Domanska and Marciniak⁴⁸ measured the surface tension of pure [HMIm][Tf₂N] at 25 °C with a value of 31.2 mN·m⁻¹ which compares with the value measured in the current

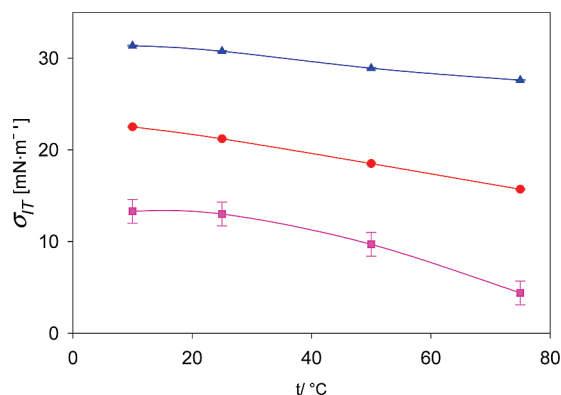


Figure 7. Interfacial tension of the saturated 1-octene (1) + [HMIm][Tf₂N] (2) system with temperature compared to the pure component surface tensions. ▲, [HMIm][Tf₂N]; ●, 1-octene; ■, IL/1-octene.

work of $30.8 \text{ mN}\cdot\text{m}^{-1}$. Coutinho and co-workers⁴⁹ measured the surface tension at 50°C with a value of $30.6 \text{ mN}\cdot\text{m}^{-1}$, compared with $28.9 \text{ mN}\cdot\text{m}^{-1}$ from this study.

3.4. Interfacial Tension. The interfacial tension of mixtures of saturated mixtures of [HMIm][Tf₂N] and 1-octene were measured at (10, 25, 50, and 75°C) and are listed in Table 6. Figure 7 illustrates that the interfacial tension decreases with temperature to a small extent at (10 and 25°C) and more significantly at the higher temperatures. Matsuda et al.⁵⁰ investigated the system of [HMIm][PF₆] saturated with hexane and decane and reported interfacial tensions at 25°C of (8.36 and $9.76 \text{ mN}\cdot\text{m}^{-1}$, respectively). These amounts are lower than the interfacial tensions reported for the ([HMIm][Tf₂N] + 1-octene) system in current study.

The interfacial tension between two liquids has been often related to their air–liquid surface tension. An expression has been proposed by van Oss⁵¹ and recently applied to IL–alkane systems:

$$\sigma_{\text{IT}}^{\text{IL-Oct}} = \sigma^{\text{IL}} + \sigma^{\text{Oct}} - 2\phi\sqrt{\sigma^{\text{IL}}\sigma^{\text{Oct}}} \quad (8)$$

where ϕ is the interaction parameter which, from other systems in the literature, is near zero for nonpolar mixtures, less than one for nonpolar/polar systems, and greater than one for polar + polar systems.⁵⁰ The regressed parameter ϕ for the 1-octene + [HMIm][Tf₂N] system at the four different temperatures is shown in Table 6. The parameter is just less than unity with a slight temperature dependence in accordance with a nonpolar/polar mixture.

4. Conclusions

ILs have a number of applications in multiphase reactions, extractions, and material processing. However, for an accurate understanding of the mass transfer, the phase equilibrium and thermodynamic properties must be understood, especially the effect of concentration. This investigation measured thermodynamic and interfacial properties for the system of 1-hexyl-3-methylimidazolium bis(trifluoromethylsulfonyl)-amide ([HMIm][Tf₂N]) and 1-octene, focusing on both the pure components and the mixtures. Liquid–liquid equilibrium data indicated that the IL exhibits minimal solubility in the 1-octene phase, whereas 1-octene has moderate solubility in the IL phase. Thus, mass transfer when the two components are mixed would occur in virtually one direction. The NRTL model satisfactorily correlated the LLE data with just a slight under-prediction of the 1-octene fraction in each phase. The density of the IL mixture decreases with increasing the concentration of 1-octene and temperature. The excess molar volume for the mixture of ILs and 1-octene is slightly negative for all isotherms. Air–liquid surface tensions of mixtures of the IL + 1-octene have been measured along with saturated interfacial tensions of the two phases.

Acknowledgment

Prof. Jerzy Petera of the Technical University of Łódź, Poland, is thanked for helpful discussions.

Literature Cited

- (1) Zhao, H.; Xia, S.; Ma, P. Use of ionic liquids as green solvents for extractions. *J. Chem. Technol. Biotechnol.* **2005**, *80* (10), 1089–1096.
- (2) Webb, P. B.; Sellin, M. F.; Kunene, T. E.; Williamson, S.; Slawin, A. M. Z.; Cole-Hamilton, D. J. Continuous flow hydroformylation of alkenes in supercritical fluid-ionic liquid biphasic systems. *J. Am. Chem. Soc.* **2003**, *125* (50), 15577–15588.
- (3) Scurto, A. M.; Aki, S.; Brennecke, J. F. CO₂ as a separation switch for ionic liquid/organic mixtures. *J. Am. Chem. Soc.* **2002**, *124* (35), 10276–10277.
- (4) Thermodynamics of ionic liquids, ionic liquid mixtures, and the development of standardized systems. *Chem. Int.* **2005**, *27* (5), 22–23.
- (5) Aghosseini, A.; Ren, W.; Scurto, A. M. Hydrogenation in Biphasic Ionic Liquid/CO₂ Systems. In *Green Chemistry and Engineering with Gas Expanded Liquids and Near-Critical Media*; Hutchenson, K. W., Scurto, A. M., Subramaniam, B., Eds.; ACS Symposium Series: Washington, DC, 2008.
- (6) Aghosseini, A.; Ren, W.; Scurto, A. M. Understanding Biphasic Ionic Liquid/CO₂ Systems for Homogeneous Catalysis: Hydroformylation. *Ind. Eng. Chem. Res.* **2009**, 95–101.
- (7) Ren, W.; Scurto, A. M. Global phase behavior of imidazolium ionic liquids and compressed 1, 1, 1, 2-tetrafluoroethane (R-134a). *AIChE J.* **2009**, *55*, 2.
- (8) Ren, W.; Scurto, A. M. Phase Equilibria of Imidazolium Ionic Liquids and the Refrigerant Gas, 1,1,1,2-Tetrafluoroethane (R-134a). *Fluid Phase Equilib.* **2009**, *286* (1), 1–7.
- (9) Roettger, D.; Nierlich, F.; Krissmann, J.; Wasserscheid, P.; Keim, W. Method for separation of substances by extraction or by washing them with ionic liquids. U.S. Patent 7,304,200, 2007.
- (10) Smith, R. S.; Herrera, P. S.; Reynolds, J. S.; Krzywicki, A. Use of ionic liquids to separate diolefins. U.S. Patent App. 10/308,307, 2002.
- (11) Aghosseini, A.; Ren, W.; Scurto, A. M. Homogeneous Catalysis in Biphasic Ionic Liquids/CO₂ Systems. *Chem. Today* **2007**, *25* (2), 40–42.
- (12) Aghosseini, A.; Ren, W.; Scurto, A. M. Understanding Biphasic Ionic Liquid/CO₂ Systems for Homogeneous Catalysis: Hydroformylation. *Ind. Eng. Chem. Res.* **2009**, *48* (9), 4254–4265.
- (13) Welton, T. Ionic liquids in catalysis. *Coord. Chem. Rev.* **2004**, *248* (21–24), 2459–2477.
- (14) Bonhôte, P.; Dias, A. P.; Papageorgiou, N.; Kalyanasundaram, K.; Grätzel, M. Hydrophobic, highly conductive ambient-temperature molten salts. *Inorg. Chem.* **1996**, *35* (5), 1168–1178.
- (15) Burrell, A. K.; Sesto, R. E. D.; Baker, S. N.; McCleskey, T. M.; Baker, G. A. The large scale synthesis of pure imidazolium and pyrrolidinium ionic liquids. *Green Chem.* **2007**, *9* (5), 449–454.
- (16) Seddon, K. R.; Stark, A.; Torres, M. J. Influence of chloride, water, and organic solvents on the physical properties of ionic liquids. *Pure Appl. Chem.* **2000**, *72* (12), 2275–2287.
- (17) Vargaftik, N. B.; Volkov, B. N.; Voljak, L. D. *International tables of the surface tension of water*; American Chemical Society and the American Institute of Physics for the National Bureau of Standards: Washington, DC, 1983.
- (18) Zepiéri, S.; Rodríguez, J.; de Ramos, A. L. L. Interfacial Tension of Alkane + Water Systems. *J. Chem. Eng. Data* **2001**, *46* (5), 1086–1088.
- (19) Prausnitz, J. M.; Lichtenthaler, R. N.; de Azevedo, E. G. *Molecular thermodynamics of fluid-phase equilibria*; Prentice Hall PTR: Upper Saddle River, NJ, 1986.
- (20) Favre, F.; Olivier-Bourbigou, H.; Commereuc, D.; Saussine, L. Hydroformylation of 1-hexene with rhodium in non-aqueous ionic liquids: how to design the solvent and the ligand to the reaction. *Chem. Commun.* **2001**, *15*, 1360–1361.
- (21) Wasserscheid, P.; Hilgers, C.; Gordon, C. M.; Muldoon, M. J.; Dunkin, I. R. Ionic liquids: polar, but weakly coordinating solvents for the first biphasic oligomerisation of ethene to higher α -olefins with cationic Ni complexes. *Chem. Commun.* **2001**, *2001* (13), 1186–1187.
- (22) Brasse, C. C.; Englert, U.; Salzer, A.; Waffenschmidt, H.; Wasserscheid, P. Ionic Phosphine Ligands with Cobaltocenium Backbone: Novel Ligands for the Highly Selective, Biphasic, Rhodium-Catalyzed Hydroformylation of 1-Octene in Ionic Liquids. *Organometallics* **2000**, *19* (19), 3818–3823.
- (23) Stark, A.; Ajam, M.; Green, M.; Raubenheimer, H. G.; Ranwell, A.; Ondruschka, B. Metathesis of 1-Octene in Ionic Liquids and Other Solvents: Effects of Substrate Solubility, Solvent Polarity and Impurities. *Adv. Synth. Catal.* **2006**, *348*, 14.
- (24) Lei, Z.; Arlt, W.; Wasserscheid, P. Separation of 1-hexene and n-hexane with ionic liquids. *Fluid Phase Equilib.* **2006**, *241* (1–2), 290–299.
- (25) Domanska, U.; Marciniak, A. Solubility of 1-Alkyl-3-methylimidazolium Hexafluorophosphate in Hydrocarbons. *J. Chem. Eng. Data* **2003**, *48* (3), 451–456.
- (26) Jiqin, Z.; Jian, C.; Chengyue, L.; Weiyang, F. Study on the separation of 1-hexene and trans-3-hexene using ionic liquids. *Fluid Phase Equilib.* **2006**, *247* (1–2), 102–106.
- (27) Meindersma, G. W.; Podt, A. J. G.; de Haan, A. B. Ternary liquid–liquid equilibria for mixtures of toluene + n-heptane + an ionic liquid. *Fluid Phase Equilib.* **2006**, *247* (1–2), 158–168.

- (28) Munson, C. L.; Boudreau, L. C.; Driver, M. S.; Schinski, W. L. Separation of olefins from paraffins using ionic liquid solutions. U.S. Patent 6 339 182, 2002.
- (29) Munson, C. L.; Boudreau, L. C.; Driver, M. S.; Schinski, W. L. Separation of olefins from paraffins using ionic liquid solutions. U.S. Patent 6 623 659, 2003.
- (30) Nebig, S.; Böltz, R.; Gmehling, J. Measurement of vapor-liquid equilibria (VLE) and excess enthalpies (H^E) of binary systems with 1-alkyl-3-methylimidazolium bis (trifluoromethylsulfonyl) imide and prediction of these properties and using modified UNIFAC (Dortmund). *Fluid Phase Equilib.* **2007**, 258 (2), 168–178.
- (31) Liebert, V.; Nebig, S.; Gmehling, J. Experimental and predicted phase equilibria and excess properties for systems with ionic liquids. *Fluid Phase Equilib.* **2008**, 268 (1–2), 14–20.
- (32) Nebig, S.; Liebert, V.; Gmehling, J. Measurement and prediction of activity coefficients at infinite dilution, vapor-liquid equilibria (VLE) and excess enthalpies (H^E) of binary systems with 1, 1-dialkylpyrrolidinium bis (trifluoromethylsulfonyl) imide using mod. UNIFAC (Dortmund). *Fluid Phase Equilib.* **2009**, 277 (1), 61–67.
- (33) Abbas, R.; Gmehling, J. Vapour-liquid equilibria, azeotropic data, excess enthalpies, activity coefficients at infinite dilution and solid-liquid equilibria for binary alcohol-ketone systems. *Fluid Phase Equilib.* **2008**, 267 (2), 119–126.
- (34) Kandil, M. E.; Marsh, K. N.; Goodwin, A. R. H. Measurement of the viscosity, density, and electrical conductivity of 1-hexyl-3-methylimidazolium bis(trifluoromethylsulfonyl) imide at temperatures between (288 and 433) K and pressures below 50 MPa. *J. Chem. Eng. Data* **2007**, 52 (6), 2382–2387.
- (35) Widegren, J. A.; Magee, J. W. Density, Viscosity, Speed of Sound, and Electrolytic Conductivity for the Ionic Liquid 1-Hexyl-3-methylimidazolium Bis (trifluoromethylsulfonyl)imide and Its Mixtures with Water. *J. Chem. Eng. Data* **2007**, 52 (6), 2331–2338.
- (36) Yaws, C. L.; Gabbula, C. *Yaws' Handbook of Thermodynamic and Physical Properties of Chemical Compounds*; Knovel: New York, 2003.
- (37) Wang, B.; Kang, Y. R.; Yang, L. M.; Suo, J. S. Epoxidation of α , β -unsaturated carbonyl compounds in ionic liquid/water biphasic system under mild conditions. *J. Mol. Catal. A: Chem.* **2003**, 203 (1–2), 29–36.
- (38) Wang, J.; Zhu, A.; Zhao, Y.; Zhuo, K. Excess molar volumes and excess logarithm viscosities for binary mixtures of the ionic liquid 1-butyl-3-methylimidazolium hexafluorophosphate with some organic compounds. *J. Solution Chem.* **2005**, 34 (5), 585–596.
- (39) Heintz, A.; Klasen, D.; Lehmann, J. K. Excess molar volumes and viscosities of binary mixtures of methanol and the ionic liquid 4-methyl-N-butylpyridinium tetrafluoroborate at 25, 40, and 50 C. *J. Solution Chem.* **2002**, 31 (6), 467–476.
- (40) Cadena, C.; Anthony, J. L.; Shah, J. K.; Morrow, T. I.; Brennecke, J. F.; Maginn, E. J. Why is CO₂ so soluble in imidazolium-based ionic liquids. *J. Am. Chem. Soc.* **2004**, 126 (16), 5300–5308.
- (41) Hanke, C. G.; Atamas, N. A.; Lynden-Bell, R. M. Solvation of small molecules in imidazolium ionic liquids: a simulation study. *Green Chem.* **2002**, 4 (2), 107–111.
- (42) Huddleston, J. G.; Visser, A. E.; Reichert, W. M.; Willauer, H. D.; Broker, G. A.; Rogers, R. D. Characterization and comparison of hydrophilic and hydrophobic room temperature ionic liquids incorporating the imidazolium cation. *Green Chem.* **2001**, 3, 156–164.
- (43) Law, G.; Watson, P. R. Surface tension measurements of N-alkylimidazolium ionic liquids. *Langmuir* **2001**, 17 (20), 6138–6141.
- (44) Dzyuba, S. V.; Bartsch, R. A. Influence of structural variations in 1-alkyl (aralkyl)-3-methylimidazolium hexafluorophosphates and bis (trifluoromethylsulfonyl) imides on physical properties of the ionic liquids. *ChemPhysChem* **2002**, 3 (2), 160–166.
- (45) Freire, M. G.; Carvalho, P. J.; Fernandes, A. M.; Marrucho, I. M.; Queimada, A. J.; Coutinho, J. A. P. Surface tensions of imidazolium based ionic liquids: Anion, cation, temperature and water effect. *J. Colloid Interface Sci.* **2007**, 314 (2), 621–630.
- (46) Kimura, T.; Fujita, M.; Ando, T. Sonochemical and photochemical reactions of bromotrichloromethane in the presence and absence of 1-alkene. *Ultrason. Sonochem.* **1999**, 6 (1–2), 93–96.
- (47) Jasper, J. J. The surface tension of pure liquid compounds. *J. Phys. Chem. Ref. Data* **1972**, 1 (4), 841–1009.
- (48) Domanska, U.; Marciniak, A. Activity coefficients at infinite dilution measurements for organic solutes and water in the ionic liquid triethylsulphonium bis (trifluoromethylsulfonyl)imide. *J. Chem. Thermodyn.* **2009**, 41 (6), 754–758.
- (49) Carvalho, P. J.; Freire, M. G.; Marrucho, I. M.; Queimada, A. J.; Coutinho, J. A. P. Surface Tensions for the 1-Alkyl-3-methylimidazolium Bis (trifluoromethylsulfonyl)imide Ionic Liquids. *J. Chem. Eng. Data* **2008**, 53 (6), 1346–1350.
- (50) Matsuda, T.; Mishima, Y.; Azizian, S.; Matsubara, H.; Takiue, T.; Aratono, M. Interfacial tension and wetting behavior of air/oil/ionic liquid systems. *Colloid Polym. Sci.* **2007**, 285 (14), 1601–1605.
- (51) van Oss, C. J. *Interface Forces in Aqueous Media*; Marcel Dekker: New York, 1994.

Received for review August 23, 2009. Accepted December 2, 2009. This work was supported by the National Science Foundation (NSF CBET-0731244 & NSF EEC-0649257). The author (A.M.S.) appreciates the support of the DuPont Young Professor Award.

JE900697W